

The following resources related to this article are available online at www.sciencemag.org (this information is current as of September 9, 2009):

Updated information and services, including high-resolution figures, can be found in the online version of this article at:

<http://www.sciencemag.org/cgi/content/full/325/5945/1236>

Supporting Online Material can be found at:

<http://www.sciencemag.org/cgi/content/full/325/5945/1236/DC1>

This article **cites 24 articles**, 6 of which can be accessed for free:

<http://www.sciencemag.org/cgi/content/full/325/5945/1236#otherarticles>

This article appears in the following **subject collections**:

Atmospheric Science

<http://www.sciencemag.org/cgi/collection/atmos>

Information about obtaining **reprints** of this article or about obtaining **permission to reproduce this article** in whole or in part can be found at:

<http://www.sciencemag.org/about/permissions.dtl>

by a factor of ~ 3 , but solar nebula mass requirements to form these configurations make them physically implausible (see SOM text for details).

Although known LPCs constrain the total population beyond $a \sim 3000$ AU, they offer little information about the relative inner and outer Oort Cloud populations because LPC production obscures orbital histories. However, inner cloud LPC production predicts the generation of $a > 20,000$ AU orbits near Jupiter and Saturn. In contrast, the outer Oort Cloud's $a > 20,000$ AU population will decrease after passing through this region. Thus, a comparison of original and future semimajor axes for a large LPC sample near $q \sim 10$ AU (analogous to that done for currently known LPCs) could provide an opportunity to distinguish between production mechanisms.

References and Notes

1. J. H. Oort, *Bull. Astron. Inst. Neth.* **11**, 91 (1950).
2. J. Heisler, S. Tremaine, *Icarus* **65**, 13 (1986).
3. P. Wiegert, S. Tremaine, *Icarus* **137**, 84 (1999).
4. J. A. Fernandez, *Astron. Astrophys.* **96**, 26 (1981).
5. H. F. Levison, M. J. Duncan, L. Dones, B. J. Gladman, *Icarus* **184**, 619 (2006).
6. Materials and methods are available as supporting material on Science Online.
7. R. Brassier, M. J. Duncan, H. F. Levison, *Icarus* **196**, 274 (2008).
8. J. Heisler, S. Tremaine, C. Alcock, *Icarus* **70**, 269 (1987).
9. H. Rickman, M. Fouchard, C. Froeschlé, G. B. Valsecchi, *Celestial Mech. Dyn. Astron.* **102**, 111 (2008).
10. V. V. Em'Yanenko, D. J. Asher, M. E. Bailey, *Mon. Not. R. Astron. Soc.* **381**, 779 (2007).
11. N. A. Kaib, T. Quinn, *Icarus* **197**, 221 (2008).
12. M. E. Brown, C. Trujillo, D. Rabinowitz, *Astrophys. J.* **617**, 645 (2004).
13. N. A. Kaib et al., *Astrophys. J.* **695**, 268 (2009).
14. E. Everhart, *Astron. J.* **72**, 716 (1967).
15. L. Dones, P. R. Weissman, H. F. Levison, M. J. Duncan, in *Comets II*, M. C. Festou, H. U. Keller, H. A. Weaver, Eds. (Univ. of Arizona Press, Tucson, 2004), pp. 153–174.
16. M. J. Duncan, R. Brassier, L. Dones, H. F. Levison, *The Role of the Galaxy in the Dynamical Evolution of Transneptunian Objects* (Univ. of Arizona Press, Tucson, AZ, 2008), pp. 315–331.
17. R. Brassier, M. J. Duncan, H. F. Levison, *Icarus* **184**, 59 (2006).
18. R. Gomes, H. F. Levison, K. Tsiganis, A. Morbidelli, *Nature* **435**, 466 (2005).
19. E. W. Thommes, M. J. Duncan, H. F. Levison, *Icarus* **161**, 431 (2003).
20. J. G. Hills, *Astron. J.* **86**, 1730 (1981).
21. P. R. Weissman, *Int. Astron. Union Symp.* **236**, 441 (2007).

22. P. Hut et al., *Nature* **329**, 118 (1987).
23. K. A. Farley, A. Montanari, E. M. Shoemaker, C. S. Shoemaker, *Science* **280**, 1250 (1998).
24. P. R. Weissman, in *Completing the Inventory of the Solar System: A Symposium Held in Conjunction with the 106th Annual Meeting of the ASP*, T. Rettig, J. M. Hahn, Eds., vol. 107 of *Astronomical Society of the Pacific Conference Series* (Astronomical Society of the Pacific, San Francisco, 1996), pp. 265–288.
25. P. J. Francis, *Astrophys. J.* **635**, 1348 (2005).
26. L. Neslusan, *Astron. Astrophys.* **461**, 741 (2007).
27. This research was funded by a NASA Earth and Space Science Fellowship and an NSF grant (AST-0709191). Our computing was performed by using Purdue Teragrid computing facilities managed with Condor scheduling software (www.cs.wisc.edu/condor). A. Morbidelli and two anonymous reviewers provided helpful comments that greatly improved our work.

Supporting Online Material

www.sciencemag.org/cgi/content/full/1172676/DC1
Materials and Methods

SOM Text

Figs. S1 to S6

References

23 February 2009; accepted 10 July 2009

Published online 30 July 2009;

10.1126/science.1172676

Include this information when citing this paper.

Recent Warming Reverses Long-Term Arctic Cooling

Darrell S. Kaufman,^{1*} David P. Schneider,² Nicholas P. McKay,³ Caspar M. Ammann,² Raymond S. Bradley,⁴ Keith R. Briffa,⁵ Gifford H. Miller,⁶ Bette L. Otto-Bliesner,² Jonathan T. Overpeck,³ Bo M. Vinther,⁷ Arctic Lakes 2k Project Members†

The temperature history of the first millennium C.E. is sparsely documented, especially in the Arctic. We present a synthesis of decadal resolved proxy temperature records from poleward of 60°N covering the past 2000 years, which indicates that a pervasive cooling in progress 2000 years ago continued through the Middle Ages and into the Little Ice Age. A 2000-year transient climate simulation with the Community Climate System Model shows the same temperature sensitivity to changes in insolation as does our proxy reconstruction, supporting the inference that this long-term trend was caused by the steady orbitally driven reduction in summer insolation. The cooling trend was reversed during the 20th century, with four of the five warmest decades of our 2000-year-long reconstruction occurring between 1950 and 2000.

As awareness of the recent rapid changes in the Arctic grows (1), so too does the need for a longer-term perspective on these changes. This study places the warming of the instrumental period against the backdrop of the past 2000 years, well beyond the 400-year scope of the last Arctic-wide synthesis of high-resolution paleoclimate data (2). Our synthesis is based on a new compilation of proxy records from Arctic lakes (3),

combined with complementary ice core and tree ring records, to form a new 2000-year-long, decadal resolved paleoclimate reconstruction for the Arctic. Lakes are distributed across the Arctic, and they contain the most accessible proxy records that consistently extend through the late Holocene. The synthesis is restricted to records longer than 1000 years because we aim to explore the long-term pattern of temperature variability at decadal scale. These records extend beyond the most recent (pre-industrial) major climate perturbation—the Little Ice Age—when most of the Arctic experienced the coldest sustained temperatures of the past 8000 years (4). In some locations, warm intervals before the Little Ice Age have been recognized during the early part of the period from 2000 to 1000 years ago, as well as during the Middle Ages (5). The spatial coherence of the warming during these intervals is not yet clear (6), but this is critical for understanding the underlying causes of change. Climate change is amplified in the Arctic (7), and warming during these historical intervals might

be more reliably detected where the temperature change exceeds the sensitivity limits of the proxies.

We compiled available proxy climate records that (i) were located north of 60°N latitude, (ii) extended back at least 1000 years, (iii) were resolved at an annual to decadal level, and (iv) were published with publicly available data (8) (table S1) (www.ncdc.noaa.gov/paleo/pubs/kaufman2009). We focused on terrestrial records because the dating resolution for most marine cores is too low to reconstruct decadal-scale variability. Our compilation includes 23 sites where lake sediment, glacial ice, and tree rings have been used as paleoclimatic archives (Fig. 1). The observed summer [June, July, and August (JJA)] temperature in the grids represented by the 23 proxy sites (Fig. 1) closely tracks the temperature for all of the land area north of 60° latitude, indicating that our proxy network accurately represents the Arctic-wide mean (8) (fig. S1). Twelve of the records are based on sedimentological and biological indicators from lakes, mainly varve properties and productivity indicators. These proxies reflect changes in summer temperatures, a primary control on physical and biological processes in lakes at high latitudes (9). Seven of the records are from glacier ice, mostly from Greenland. These rely on oxygen isotopes, which reflect a combination of the temperature and moisture transport history of the snow that accumulated on the ice sheet throughout the year (10). Four of the records are based on the width of tree rings, which have been interpreted primarily as a proxy for warm-season temperature, and were processed using the regional curve standardization procedure to help preserve the long-term variability (11). The chronologies for nearly all records are based on annual layer counting, and most authors report accuracies to within $\pm 2\%$. Some of the lake records used radioisotopes to model downcore trends in sedimentation rate, with uncertainties within $\pm 10\%$ for the past 2000 years.

¹School of Earth Sciences and Environmental Sustainability, Northern Arizona University, Flagstaff, AZ 86011, USA. ²Climate and Global Dynamics Division, National Center for Atmospheric Research, Boulder, CO 80305, USA. ³Department of Geosciences, University of Arizona, Tucson, AZ 85721, USA. ⁴Department of Geosciences, University of Massachusetts, Amherst, MA 01003, USA. ⁵Climatic Research Unit, University of East Anglia, Norwich NR4 7TJ, UK. ⁶Institute of Arctic and Alpine Research, University of Colorado, Boulder, CO 80309, USA. ⁷Niels Bohr Institute, University of Copenhagen, 2100 Copenhagen, Denmark.

*To whom correspondence should be addressed. E-mail: darrell.kaufman@nau.edu

†These authors and their affiliations are presented at the end of this paper.

Our “composite-plus-scale” synthesis (12) focuses on 10-year-mean temperatures to accommodate records that are not annually resolved and to minimize the effect of minor age uncertainties. In addition, the coherence of the regional climate signal is greater on decadal time scales than inter-annually (13). Each record was subdivided into 200 10-year intervals, and the average series were standardized to a mean of zero and unit variance relative to the 820-year period (980 to 1800) common to all records (table S2). The records were then composited by averaging the standardized series without weighting. The 10-year-mean proxy values from the 19 records that extend into the late 20th century (Fig. 2) were used to generate a least-squares linear regression that scales the proxy data to the Arctic-wide summer temperature ($r^2 = 0.79$, $P < 0.01$) (8). We used the spatially averaged summer temperature for all land area north of 60° latitude from the CRUTEM3 data series (14).

Among the most striking features of our composite temperature reconstruction is a cooling from 1 C.E. to 1900 C.E. (Fig. 3). The cooling trend is especially clear in records from ice and lakes (Fig. 3A). For trees, only three records extend back before 720, which is not enough to determine a reliable trend. The cooling trend is based on the 17 records that extend back two millennia (Fig. 3B). The other six records that extend back to at least 980 track the longer-term records for the period of overlap ($r^2 = 0.23$, $P < 0.01$). Least-squares linear regression yields a cooling trend of $-0.22^\circ \pm 0.06^\circ\text{C}$ per 1000 years (8) (Fig. 3C).

Principal components (PC) analysis was used to extract the dominant mode of variability from the 15 standardized records that extend from 1 C.E. to 1900 C.E. (table S1). The leading mode explains 17% of the variance of all records, and its time series is similar to the simple composite of the records for this period ($r^2 = 0.84$, $P < 0.01$). All records are positively correlated with PC1, indicating that the trends are predominantly of the same sign over the 1900-year period.

Because the unweighted composite and the PC of the records at 10-year intervals could be skewed by extreme values from a few records, we generated an alternative composite record using the approach of Osborn and Briffa (15). For this procedure, the number of available records for each 10-year interval with a proxy value that exceeded either +1 or -1 SD was tallied, and the difference in the proportion of records that exceeded these thresholds was calculated by subtraction. The resulting time series shows a monotonic decrease similar to the mean composite and to the PC values (Fig. 3E).

The millennial-scale cooling trend is consistent with other proxy evidence showing that summer temperatures across the Arctic reached their maximum during the first half of the present interglaciation (between about 10,000 and 6000 years ago), then cooled into neoglaciation (4). For example, summer melt became less frequent on ice caps in northeastern Canada (16), the tree line retreated southward across northern Eurasia (17), herbaceous tundra expanded in Fennoscandia (18), and gla-

ciers expanded in mountains across the Arctic (19). Proxy data from the western hemisphere of the Arctic indicate that summer temperatures were $1.6^\circ \pm 0.8^\circ\text{C}$ higher during the Holocene thermal maximum (HTM) than the average of the 20th century (20). The timing of the HTM transgressed from west to east across the North American Arctic but generally peaked around 7500 years ago, suggesting a post-HTM cooling rate between -0.11° and -0.32°C per 1000 years. This compares well with the average cooling rate of $-0.22^\circ \pm 0.06^\circ\text{C}$ per 1000 years derived here for our 2000-year time series of Arctic summer temperature (Fig. 3C).

The millennial-scale cooling trend in our temperature reconstruction correlates with the reduction in summer insolation, which was primarily driven by the precession of the solstices around Earth’s elliptical orbit. Over the past 2000 years, summer (JJA) insolation at the top of the atmosphere decreased by about 6 W m^{-2} at 65°N (Fig. 3F) (21). The forcing was weaker at lower latitude, especially for the early summer. The decrease in insolation during the summer was partly counterbalanced by an increase during the winter, although winter conditions have little influence on the proxy climate indicators.

Fig. 1. Locations of the proxy climate records included in the synthesis. Map colors indicate trends in summer (JJA) temperature between 1958 and 2000 from the ERA-40 data series (34). Large and small symbols indicate records that extend back to 2000 years ago (2 ka) and to at least 1000 years ago, respectively. Site numbers are keyed to table S1.

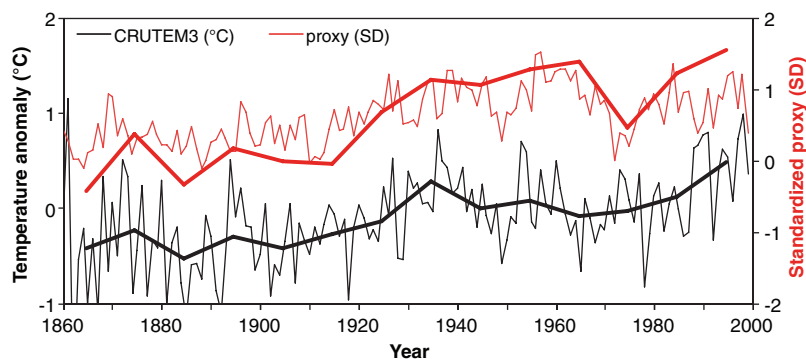
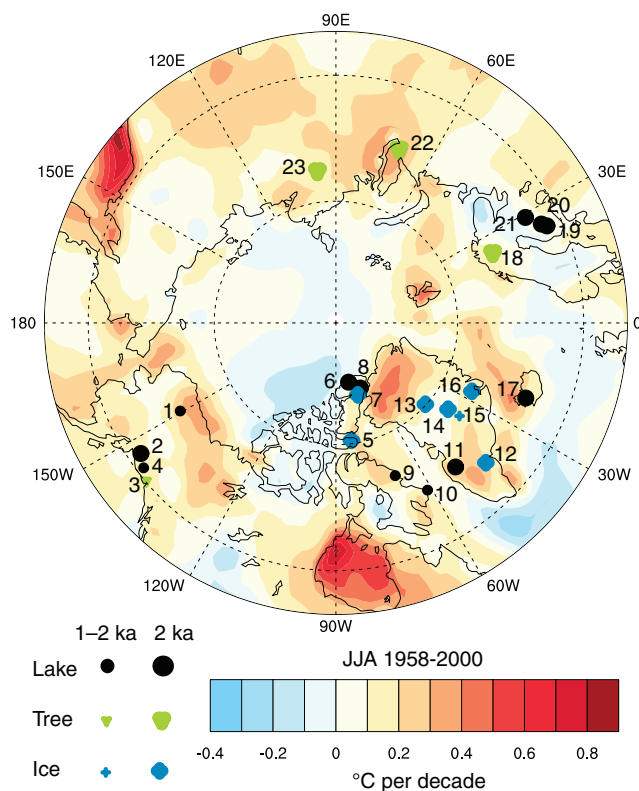


Fig. 2. Comparison between Arctic-wide mean summer (JJA) temperature anomalies relative to the period 1961–1990 based on the CRUTEM3 data series (14) and mean standardized proxy values (SD units). The annual proxy values (narrow red line) are averaged from the 10 sites with annually resolved time series that extend into the late 20th century, whereas the 10-year-mean proxy values (bold red line) are based on all 19 sites with records that extend through the 20th century. Ten-year means (bold lines) were used to derive a regression equation to scale our new proxy record to summer temperature (8).

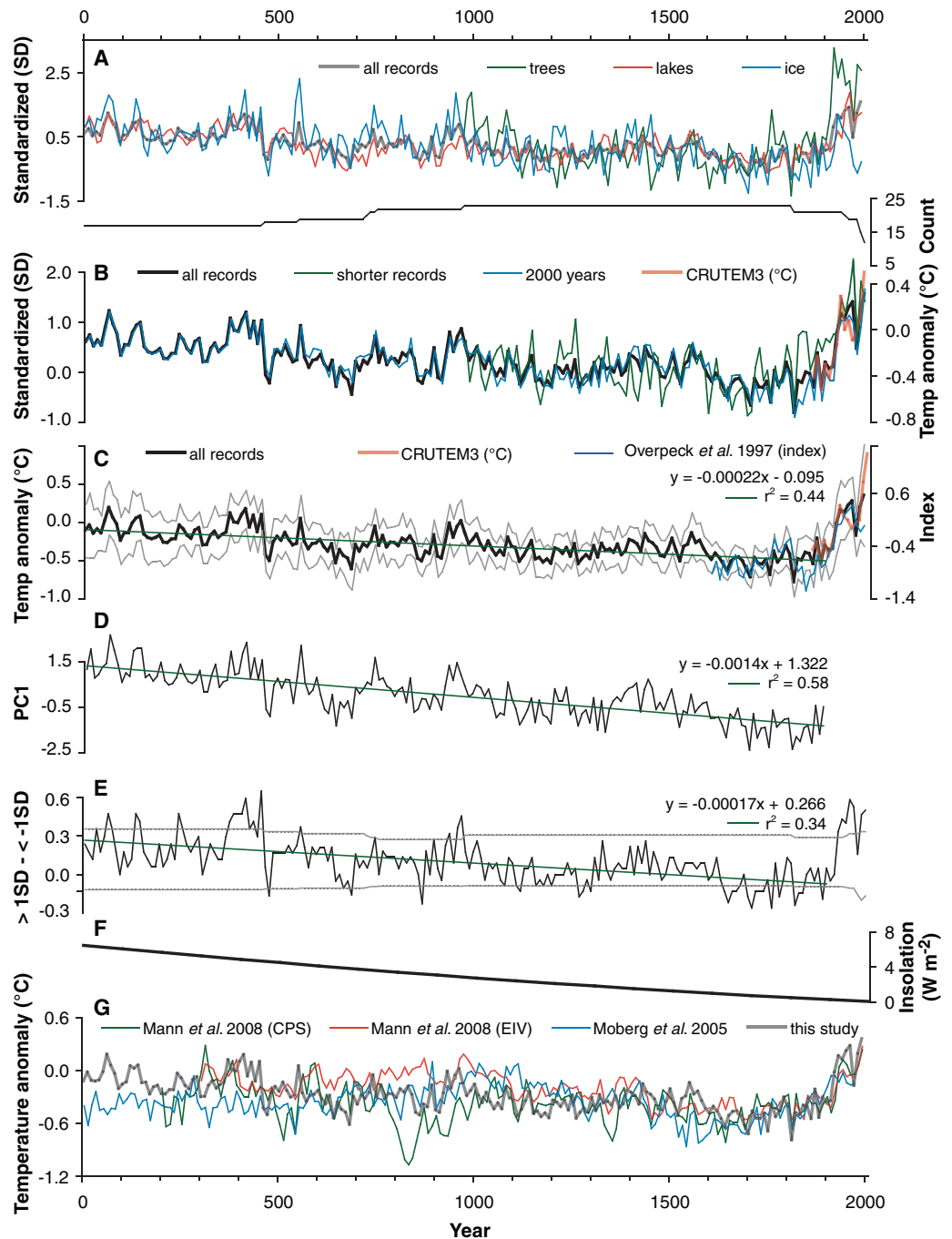
Assuming that the overall cooling since the HTM was ultimately caused by the decrease in summer insolation (19), it seems likely that this insolation anomaly of +1.4% relative to the present at 65°N was amplified by climate feedbacks (22). The strongest positive feedbacks in the Arctic are related to changes in terrestrial snow and sea-ice cover, which (like our climate proxies themselves) are sensitive to warm-season temperatures and respond rapidly to summer insolation anomalies. As sea ice expanded after the HTM (23), both the amount of solar energy absorbed by the ocean surface waters and the transfer of heat from the surface water to the atmosphere were diminished. The expansion of tundra into areas formerly cov-

ered by shrubs or forest may have further contributed to the terrestrial snow and land-cover albedo feedback (24).

These sea-ice, snow, and terrestrial feedbacks were represented in a transient, mid-late Holocene simulation with the Community Climate System Model (CCSM3) (8, 25). For the period from 5600 to 3600 years ago, orbital forcing was the strongest time-varying forcing of this simulation. Results from this simulation show that the relation between summer insolation and temperature in the model is the same as for the proxy reconstruction, thereby supporting the connection between the Arctic summer cooling trend and the orbitally driven reduction in summer insolation (Fig. 4).

In contrast to our regional reconstruction, recently published syntheses of the Northern Hemisphere average temperature do not show an overall 1900-year-long cooling trend (26, 27) (Fig. 3G). Rather, they are dominated by centennial-scale fluctuations, with little indication that the first 1000 years C.E. was warmer than the millennium that followed. The centennial-scale anomalies around the long-term trend in our high-latitude reconstruction appear to correspond with the temporal structure from the Northern Hemisphere as a whole. The period from about 450 to 700 was generally cooler than the linear trend, and the period from 900 to 1050 tended to be warmer. In good agreement with other reconstructions (28), the coldest interval

Fig. 3. (A and B) Composite of 23 high-resolution proxy climate records from the Arctic. Values are 10-year means standardized relative to the reference period of 980 to 1800. (A) Records subdivided by source of proxy information: trees, ice, and lakes, with the running count of records. (B) Records subdivided by those that extend 2000 years ($n = 17$) versus shorter records ($n = 6$), along with the 10-year-mean Arctic-wide summer temperature through 2000 from the CRUTEM3 data series (14) (red line). (C) Mean of all records transformed to summer temperature anomaly relative to the 1961–1990 reference period, with first-order linear trend for all records through 1900 (green line), the 400-year-long Arctic-wide temperature index of Overpeck *et al.* (2) (blue curve; 10-year means), and the 10-year-mean Arctic temperature through 2008 (red line). Gray lines encompass ± 2 standard errors of the proxy values as evaluated for each 10-year interval. (D) Time series of PC1 based on the 15 records that extend from 1 C.E. to 1900 C.E., showing a strong first-order trend. (E) Difference in the fractional proportion of records that exceed ± 1 SD for each 10-year interval. Gray lines are 95th percentile of distributions determined by 10,000 Monte Carlo realizations of shifting the time series randomly in time [as in (15)]. (F) Change in summer (JJA) insolation at 65°N latitude relative to the 20th century (21). (G) Northern Hemisphere average proxy temperature anomalies (10-year means) reconstructed by Mann *et al.* (26) on the basis of two approaches (CPS, composite plus scale; EIV, error in variables) and by Moberg *et al.* (27). Our Arctic regional reconstruction is overlaid in gray.



Downloaded from www.sciencemag.org on September 9, 2009

occurred between 1600 and 1850. The Arctic record therefore supports the centennial-scale variations documented elsewhere, which can be reasonably explained by solar irradiance and volcanic forcing (29).

Strong warming in the 20th century contrasts sharply with the preceding cooling trend. An Arctic summer temperature of -0.5°C (relative to the period 1961–1990) might have been expected by the mid-20th century on the basis of a simple forward projection of the linear trend in the proxy data for the period from 1 C.E. to 1900 C.E. (Fig. 3C). Instead, our reconstruction indicates that temperatures increased to $+0.2^{\circ}\text{C}$ by 1950. This shift correlates with the rise in global average temperature, which coincided with the onset of major anthropogenic changes in global atmospheric composition, the absence of major volcanic eruptions, and changes in solar irradiance (30). During the early 20th century, warming in the Arctic was enhanced relative to the global average, likely reflecting a combination of natural variability (31) and positive

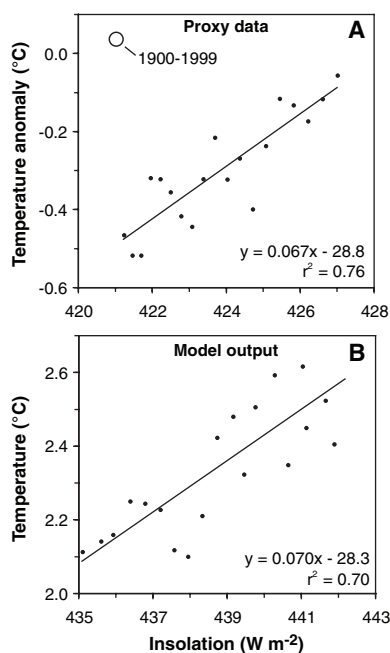


Fig. 4. Sensitivity of Arctic summer (JJA) temperature to orbital forcing, as inferred from (A) our proxy-based reconstruction, and (B) a 2000-year simulation by the Community Climate System Model (CCSM3). For (A), temperatures are 100-year-mean JJA values relative to the 1961–1990 reference period. The 20th century (open circle) is anomalous with respect to the trend defined by the previous 1900 years. The slope of the least-squares regression implies a regional sensitivity of $0.07^{\circ} \pm 0.02^{\circ}\text{C}$ per W m^{-2} for the proxy-based estimate. Insolation is average JJA at 65°N from Berger and Loutre (21). For (B), temperatures are from CCSM3-simulated (8) 100-year-mean JJA area-averaged values for land north of 60°N latitude. The model-derived sensitivity is also $0.07^{\circ} \pm 0.02^{\circ}\text{C}$ per W m^{-2} . Insolation is average JJA at 65°N from the CCSM3 simulation. Axis scales in (A) and (B) are the same for visual comparison of regression slope; values differ because (B) is based on model conditions for the period from 5600 to 3600 years ago.

feedbacks that amplified the radiative forcing (7). During the late 20th century, our proxy-inferred summer temperatures were the warmest of the past two millennia, with four of the five warmest decades of our 2000-year-long reconstruction occurring between 1950 and 2000. In recent years, the magnitude of the warming seems to have emerged above the natural variability, consistent with the sharp reduction in summer sea-ice cover (32) and the rapid increase in biological activity in circum-Arctic lakes (9).

The strongest trend in our proxy temperature reconstruction is the millennial-scale cooling of $-0.22^{\circ} \pm 0.06^{\circ}\text{C}$ per 1000 years. The cooling corresponds with the slow reduction in summer insolation at high northern latitudes, driven by orbital forcing and enhanced by positive feedbacks that amplified the forcing more strongly than at lower latitudes. Summer insolation correlates with summer temperature in our proxy reconstruction and in a 2000-year climate simulation by CCM3 (Fig. 4). Orbital driven summer insolation continued to decrease through the 20th century, implying that summer temperatures should have continued to cool. Instead, the shift to higher temperatures during the 20th century reversed the millennial-scale cooling trend. The warming during the 20th century (and first decade of the 21st century) contrasts sharply with the millennial-scale cooling, with the last half-century being the warmest of the past two millennia. Our synthesis, together with the instrumental record, suggests that the most recent 10-year interval (1999–2008) was the warmest of the past 200 decades. Temperatures were about 1.4°C higher than the projected value based on the linear cooling trend and were even more anomalous than previously documented.

References and Notes

1. *Arctic Climate Impact Assessment* (Cambridge Univ. Press, Cambridge, 2005).
2. J. Overpeck *et al.*, *Science* **278**, 1251 (1997).
3. Special Issue: Late Holocene Climate and Environmental Change Inferred from Arctic Lake Sediment, D. S. Kaufman, Ed., *J. Paleolimnol.* **41** (no. 1) (2009).
4. G. H. Miller *et al.*, in *Past Climate Variability and Change in the Arctic and at High Latitudes, CCSM Synthesis and Assessment Product 1.2* (www.climate-science.gov/Library/sap/sap1-2/final-report/default.htm), chapter 4 (2009).
5. H. H. Lamb, *Climate, History and the Modern World* (Routledge, London, 1995).
6. T. J. Crowley, *Science* **289**, 270 (2000).
7. M. C. Serreze, J. A. Francis, *Clim. Change* **76**, 241 (2006).
8. See supporting material on Science Online.
9. J. P. Smol *et al.*, *Proc. Natl. Acad. Sci. U.S.A.* **102**, 4397 (2005).
10. J. Jouzel *et al.*, *J. Geophys. Res.* **102**, 26471 (1997).
11. K. R. Briffa *et al.*, *Philos. Trans. R. Soc. London Ser. B* **363**, 2269 (2008).
12. T. C. K. Lee, F. W. Zwiers, M. Tsao, *Clim. Dyn.* **31**, 263 (2008).
13. P. D. Jones, K. R. Briffa, in *Climatic Variations and Forcing Mechanisms of the Last 2000 Years*, P. D. Jones, R. S. Bradley, J. Jouzel, Eds. (Springer, New York, 1995), pp. 625–643.
14. Climatic Research Unit CRUTEM3 temperature data are described in (33) and are available at www.cru.uea.ac.uk/cru/data/temperature.
15. T. J. Osborn, K. R. Briffa, *Science* **311**, 841 (2006).
16. D. A. Fisher, R. M. Koerner, N. Reeh, *Holocene* **5**, 19 (1995).
17. G. M. MacDonald *et al.*, *Quat. Res.* **53**, 302 (2000).
18. H. Seppä, H. J. B. Birks, *Quat. Res.* **57**, 191 (2002).
19. H. Wanner *et al.*, *Quat. Sci. Rev.* **27**, 1791 (2008).
20. D. S. Kaufman *et al.*, *Quat. Sci. Rev.* **23**, 529 (2004).
21. A. Berger, M. F. Loutre, *Quat. Sci. Rev.* **10**, 297 (1991).
22. M. W. Kerwin *et al.*, *Paleoceanography* **14**, 200 (1999).

23. J. H. England *et al.*, *Geophys. Res. Lett.* **35**, L19502 (2008).
24. J. A. Foley, J. E. Kutzbach, M. T. Coe, S. Levis, *Nature* **371**, 52 (1994).
25. B. L. Otto-Bliesner *et al.*, *J. Clim.* **19**, 2567 (2006).
26. M. E. Mann *et al.*, *Proc. Natl. Acad. Sci. U.S.A.* **105**, 13252 (2008).
27. A. Moberg, D. M. Sonechkin, K. Holmgren, N. M. Datsenk, W. Karlén, *Nature* **433**, 613 (2005).
28. E. Jansen *et al.*, in *Climate Change 2007: The Physical Science Basis. Contribution of Working Group I to the Fourth Assessment Report of the Intergovernmental Panel on Climate Change*, S. Solomon *et al.*, Eds. (Cambridge Univ. Press, Cambridge, 2007), pp. 433–497.
29. C. M. Ammann, F. Joos, D. S. Schimel, B. L. Otto-Bliesner, R. A. Tomas, *Proc. Natl. Acad. Sci. U.S.A.* **104**, 3713 (2007).
30. G. C. Hegerl *et al.*, in *Climate Change 2007: The Physical Science Basis. Contribution of Working Group I to the Fourth Assessment Report of the Intergovernmental Panel on Climate Change*, S. Solomon *et al.*, Eds. (Cambridge Univ. Press, Cambridge, 2007), pp. 663–745.
31. L. Bengtsson, V. A. Semenov, O. M. Johannessen, *J. Clim.* **17**, 4045 (2004).
32. M. C. Serreze, A. P. Barrett, J. C. Stroeve, D. N. Kindig, M. M. Holland, *Cryosphere* **3**, 11 (2009).
33. P. Brohan, J. J. Kennedy, I. Harris, S. F. B. Tett, P. D. Jones, *J. Geophys. Res.* **111**, D12106 (2006).
34. ERA-40 Archive (<http://dss.ucar.edu/pub/era40>).
35. Supported by the Arctic System Science Program of NSF [grants ARC-0455043 (D.S.K.), 0454959 (R.S.B.), 0455025 (G.H.M.), 0450938 (J.T.O.), and 0454930 (B.L.O.-B.)]. NCAR is funded by NSF. We thank our collaborators on the ARCS 2k Project (www.arcus.org/synthesis2k) for their contributions, and M. Hughes, K. Kreutz, and reviewers for their input. NOAA Paleoclimatology assisted with data management.

Arctic Lakes 2k project members include the primary contributors to (3): M. Abbott,¹ Y. Axford,² B. Bird,¹ H. J. B. Birks,³ A. E. Bjune,⁴ J. Briner,⁵ T. Cook,⁶ M. Chipman,⁷ P. Francus,⁸ K. Gajewski,⁹ A. Geirsdóttir,¹⁰ F. S. Hu,¹¹ B. Kutchko,¹ S. Lamoureux,¹² M. Loso,¹³ G. MacDonald,¹⁴ M. Peros,⁹ D. Porinchu,¹⁵ C. Schiff,¹⁶ H. Seppä,¹⁷ E. Thomas⁵

¹Department of Geology and Planetary Science, University of Pittsburgh, Pittsburgh, PA 15260, USA. ²Institute of Arctic and Alpine Research and Department of Geological Sciences, University of Colorado, Boulder, CO 80309, USA. ³Bjerknes Centre for Climate Research and Department of Biology, University of Bergen, Allégaten 41, 5007 Bergen, Norway. ⁴Bjerknes Centre for Climate Research, University of Bergen, Allégaten 41, 5007 Bergen, Norway. ⁵Department of Geology, State University of New York, Buffalo, NY 14260, USA. ⁶Climate System Research Center, Department of Geosciences, University of Massachusetts, Amherst, MA 01003, USA. ⁷Department of Geology, University of Illinois, Urbana, IL 61801, USA. ⁸Institut National de la Recherche Scientifique, Centre Eau, Terre et Environnement, Québec G1K 9A9, Canada. ⁹Laboratory for Paleoclimatology and Climatology, Department of Geography, University of Ottawa, Ottawa, Ontario K1N 6N5, Canada. ¹⁰Institute of Earth Sciences and Department of Geosciences, University of Iceland, Reykjavík 101, Iceland. ¹¹Department of Plant Biology, University of Illinois, Urbana, IL 61801, USA. ¹²Department of Geography, Queen's University, Kingston, Ontario K7L 3N6, Canada. ¹³Environmental Science Department, Alaska Pacific University, Anchorage, AK 99508, USA. ¹⁴Department of Geography and Department of Ecology and Evolutionary Biology, University of California, Los Angeles, CA 90095, USA. ¹⁵Department of Geography, Ohio State University, Columbus, OH 43210, USA. ¹⁶School of Earth Sciences and Environmental Sustainability, Northern Arizona University, Flagstaff, AZ 86011, USA. ¹⁷Department of Geology, University of Helsinki, FIN-00014 Helsinki, Finland.

Supporting Online Material

www.sciencemag.org/cgi/content/full/325/5945/1236/DC1
SOM Text
Figs. S1 to S3
Tables S1 and S2
References

24 March 2009; accepted 22 June 2009
10.1126/science.1173983